

# Quantum efficiency determination of a novel CMOS design for fast imaging applications in the extreme ultraviolet

Stefan Herbert\*,<sup>1,2</sup> Matus Banyay,<sup>1,2</sup> Aleksey Maryasov,<sup>1,2</sup> Frank Hochschulz,<sup>3</sup>

Uwe Paschen,<sup>3</sup> Holger Vogt,<sup>3</sup> Larissa Juschkin<sup>1,2</sup>

<sup>1</sup>RWTH Aachen University Chair for Technology of Optical Systems, Steinbachstr. 15, 52074 Aachen, Germany

<sup>2</sup>JARA – Fundamentals of Future Information Technology, Research Centre Jülich 52425, Germany

<sup>3</sup>Fraunhofer Institute for Microelectronic Circuits and Systems IMS, Finkenstr. 61, 47057 Duisburg, Germany

\*Corresponding author: stefan.herbert@ilt.fraunhofer.de

*We present quantum efficiency and quantum yield measurements of novel deep optical stack etched XUV CMOS photo diodes of different sizes and derive future potentials. Quantum efficiencies between 24 and 50% at 13.5 nm were achieved. Variations in quantum efficiency and quantum yield measurement results were analyzed.*

**Keywords:** defect inspection, EUV microscopy, EUV CMOS

Extreme ultraviolet (XUV) light has gained major interest by the semiconductor industry because of the potential to cost-efficiently print smaller features than the current deep ultraviolet lithography. Technological progress has created numerous XUV applications that require image sensors. However, many techniques are restricted in their potential throughput by the slow read out speeds of established back-thinned charge coupled devices (CCD). In contrast, complementary metal oxide semiconductor (CMOS) technology offers the benefit of high read out speeds, free selectable sensor geometries and no blooming- and smear effects, but generally is not sensitive to XUV. Rapid read out rates are needed for numerous applications, mostly in inspection tools for quality control [1] in the visible spectral range (VIS) but also in the emerging field of Extreme Ultraviolet Lithography (EUVL), where 13.5 nm radiation is

used. An example is the defect inspection of mask blanks [2, 3]. The penetration depth of extreme ultraviolet (XUV, 4 – 40 nm) radiation for normal incidence is on the order of 10 – 100 nm [4], which impedes front side illumination of common detectors. Currently, this problem is circumvented by the use of back-thinned and backside illuminated sensors [5]. In this paper, a CMOS image sensor process extension called deep optical stack etching (DOSE) based on pure CMOS fabrication tools is presented, which enables the detection of front side incident XUV radiation with a high efficiency. First diode prototypes of different sizes (one of 300x300  $\mu\text{m}^2$ , 5x5 array of 60x60  $\mu\text{m}^2$ , 43x43 array of 7x7  $\mu\text{m}^2$  photo diodes) have been fabricated. Their sensitivity to XUV radiation has been determined by the PTB (Physikalisch Technische Bundesanstalt) at the XUV beamline at BESSY II, Berlin – which serves as the European standard for XUV metrology [6,7]. The CMOS process used for the fabrication of the photo diodes is a 0.35  $\mu\text{m}$  LOCOS (Local Oxidation of Silicon) process featuring two polysilicon and four metal layers using 200 mm wafers. The photo diodes are n-well implantations on a p-doped epitaxial layer. The DOSE process is based on a polysilicon stopping layer on top of a thermal oxide covering the photo diodes. In combination with the pad etching step at the very end of the CMOS process the complete optical stack on top of this stopping layer is removed using reactive ion etching (RIE). Subsequently the poly stopping layer is removed using decoupled plasma source RIE, leaving only a thin thermal oxide on top of the photo active regions. The DOSE process is shown schematically in Fig. 1. The remaining

thermal oxide serves as an etch stop for the etching of the polysilicon stopping layer. The remaining thermal oxide features a thickness of ~50 nm for the presented photo diodes. The absorption of this layer affects the spectral sensitivity. At 13.5 nm its absorption is ~40%. To characterize the sensitivity of a photo diode or image sensor, the quantum efficiency  $QE$  and quantum yield  $QY$  are determined. The  $QY$  is the amount of electrons detected per impinging photon (1).

$$QY(\lambda) = \frac{n_{e,det}}{n_{ph}} \quad (1)$$

Where  $n_{e,det}$  is the number of detected electrons and  $n_{ph}$  is the number of impinging photons. The maximum detectable number of electrons per impinging photon (ideal  $QY$ ) is the number of generated electron hole pairs per absorbed photon  $\eta(\lambda)$  and results from the ratio of the photon's energy and the effective energy bandgap of the detector material. The  $QE$  can be understood as the combined probability that a photon is absorbed in the active region and that a generated electron hole pair is detected. It is the  $QY$  divided by the number of electron hole pairs  $\eta(\lambda)$ , generated per photon, absorbed in the photosensitive region. This can be calculated using the effective energy bandgap of silicon for short wavelengths (2).

$$\eta(\lambda) = \frac{E_{ph}(\lambda)}{E_{gap}(\lambda)} \quad (2)$$

In the XUV region this bandgap is about  $E_{gap}(\lambda)=3.7\text{eV}$  [8]. The built in potential of the PN junction separates the electron hole pairs to generate the photo current  $I_{ph}(\lambda)$ . It was corrected by the dark current of the photo diode and measured without externally biasing the diode. By using apertures the photon beam size irradiating the photo diode arrays was controlled to be smaller than the array size. The photo diode arrays were then positioned in a way that the beam was completely inside the array. For a correct determination of a photo diode's sensitivity the ratio of the photo active area to the full array area (fill factor  $F$ ) has been considered in the calculation of the  $QY$  and  $QE$ . The photo active area of the photo diodes was determined using SEM cross sections (shown for example for  $7 \times 7 \mu\text{m}^2$  photo diodes in Fig. 2). The photo active region can be estimated by the distance between the sidewalls at the upper edge, obtained from SEM images. The sidewall angle of the photo active regions is around  $85^\circ$ . At this angle the incident XUV radiation is being highly reflected, so that the walls deflect the incident radiation to the photo sensitive region. This results in increased effective fill factors, which are 0.56 for the  $60 \times 60 \mu\text{m}^2$  array and 0.06 for the  $7 \times 7 \mu\text{m}^2$  arrays. As the diode arrays completely covered the photon beam, only the beam's radiant flux  $P_b(\lambda)$  is needed for the calculation of the  $QY$  and  $QE$ . It was obtained from measurements with a calibration diode and the ratio of the electron beam currents during calibration and measurement. The resulting formula for the  $QE$  is (3).

$$QE(\lambda) = \frac{E_{ph}(\lambda) \cdot I_{ph}(\lambda)}{e \cdot P_b(\lambda) \cdot F \cdot \eta(\lambda)} \cdot 100\%. \quad (3)$$

Where  $E_{ph}(\lambda)$  is the photon energy,  $e$  the elementary charge and  $\lambda$  is the wavelength.

The resulting  $QE$  and  $QY$  are shown in Fig. 3. To investigate process nonuniformities over the wafer geometry, especially from the wafer center to the wafer edge, photo diodes from two different wafer locations have been investigated. Measurements of the  $60 \times 60 \mu\text{m}^2$  photo diodes from the wafer center could not be conducted due to synchrotron beam time limitations. For comparison the  $QE$  and  $QY$  of a state-of-the-art back-thinned e2v sensor CCD47-10 [9] are shown, which has been investigated previously [10]. Furthermore, a simulation of the  $QE$  is shown, which is based on a simulation of the optical effects using the transfer matrix formalism [11] and a calculation of the generated charge carriers in the photo active volume of the diode. Recombination effects are not regarded in the simulation. The results show a  $QE$  in the range of 24 to 50% at 13.5 nm which is slightly lower than the  $QE$  from the back-thinned CCD sensor from e2v (58%). The  $60 \times 60 \mu\text{m}^2$  and  $7 \times 7 \mu\text{m}^2$  photo diodes from the wafer edge show a slightly higher sensitivity than the other photo diodes at 13.5 nm. This can be explained by the higher etch rate at the wafer edge combined with a higher etch rate near the sidewalls of an etching, due to the reflection of reactive ions. This damaged the thermal oxide and removed it partly in photo active areas (Fig. 4).

By comparing  $QE$  simulations of different thermal oxide thicknesses (Fig. 5) to the measurement results, the improved sensitivity of the  $60 \times 60 \mu\text{m}^2$  photo diodes from the wafer edge is estimated to correspond to a reduction of the thermal oxide by ~15 nm or a fraction of ~33%. Hereby recombination effects have been taken into account. For the  $7 \times 7 \mu\text{m}^2$  photo diodes from the wafer edge these values are ~25 nm or ~50%. An exemplary application for an XUV sensitive detector with a high readout speed is actinic mask blank defect inspection for EUVL. A mask blank inspection demonstrator, which operates in dark field mode, is described in more detail elsewhere [2]. One of the critical requirements for a mask blank inspection tool is a total scan time per blank ( $150 \times 150 \text{ mm}$ ) of 45 min. The high scan speed places a demand on the optical flux, the mechanics of sample movement and on the read out speed of the detector. Up to date, the bottleneck of these systems is an insufficient CCD read out speed, especially for full frame read out systems. The fastest readout of unsynchronized CCD cameras can be achieved by Frame Transfer CCDs, with a read out speed of around 10 fps ( $1024 \times 1024$  pixels). The complex synchronization between the readout charge transfer in the CCD and the sample movement (TDI, Time Delay and Integration) enables to achieve even higher read out speeds, but is still not sufficiently fast. According to the recent review by Goldberg and Mochi [12] the fastest solution of actinic mask blank inspection has been achieved by using TDI mode by Terasawa et al. [3]. With that setup a scan speed of 0.16 blanks per hour has been reported. To close the gap between current scan speeds and industrial requirements, new detector designs like the presented DOSE

photo diodes are mandatory. The photo diodes based on the DOSE process show promising results that can significantly improve EUV imaging systems in the future in terms of speed while maintaining acceptable quantum efficiency. Current work includes the reduction of the thermal oxide thickness to  $\sim 10$  nm and better etch-control to avoid the damaging of the thermal oxide at the wafer edge. Using this optimized process, an image sensor is planned. Anticipated features are a resolution of 1280x960 pixels, a pixel pitch of 12  $\mu\text{m}$ , a fill factor of  $\sim 50\%$ , an average QE of 30% at 13.5 nm and a maximum frame rate of 200 fps. With such a high scan speed, a flexible sensor architecture and no blooming- and smear effect, the DOSE image sensor shows potential for numerous XUV applications, e.g. quality control or reflectometry.

We thank the PTB, in particular Dr. Laubis and Dr. Scholze, for their support and collaboration. Furthermore we acknowledge the support of COST Action MP0601 “Short Wavelength Laboratory Sources”.

#### REFERENCES

- [1] I. I. Grulkowski, M. Gora, M. Szkulmowski, I. Gorczynska, D. Szlag, S. Marcos, A. Kowalczyk and M. Wojtkowski, “Anterior segment imaging with Spectral OCT system using a high-speed CMOS camera”, *Optics Express* Vol. 17, No. 6, pp. 4842-4858, 2009
- [2] S. Herbert, A. Maryasov and L. Juschkin, “Defect Inspection with an EUV Microscope”, *Proc. SPIE*, pp. 75450O-75450O-9, 2010
- [3] T. Terasawa, T. Yamane, T. Tanaka, O. Suga, T. Kamo and I. Mori, “Actinic phase defect detection and printability analysis for patterned EUVL mask”, *Proc. SPIE*, pp. 763602-763602-10, 2010
- [4] A. Theuwissen, Dordrecht: Kluwer, “Solid-State Imaging with Charge-Coupled Devices”, pp. 131-133, 1995
- [5] F.M. Li and A. Nathan, “CCD Image Sensors in Deep-Ultraviolet” Springer pp. 35-37, 2005
- [6] [www.helmholtz-berlin.de/zentrum/grossgeraete/index\\_en.html](http://www.helmholtz-berlin.de/zentrum/grossgeraete/index_en.html)
- [7] F. Scholze, J. Tümmeler and G. Ulm, “High-accuracy radiometry in the EUV range at the PTB soft x-ray beamline”, *Metrologia* 40, pp. 224-228, 2003
- [8] M. Krumrey and E. Tegeler, “Self-calibration of semiconductor photodiodes in the soft x-ray region”, *Rev. Sci. Instrum.* 63, pp. 797-801, 1991
- [9] [www.e2v.com](http://www.e2v.com)
- [10] M. Banyay, S. Brose and L. Juschkin, “Line image sensors for spectroscopic applications in the extreme ultraviolet”, *Meas. Sci. Technol.* 20 105201, 5pp, 2009
- [11] Knittl, Z., “Optics of Thin Films”, pp. 37-46, Wiley, 1976
- [12] K. A. Goldberg and I. Mochi, “Wavelength-specific reflections: A decade of extreme ultraviolet actinic mask inspection research”, *J. Vac. Sci. Technol. B* 28, pp. C6E1-C6E10, 2010

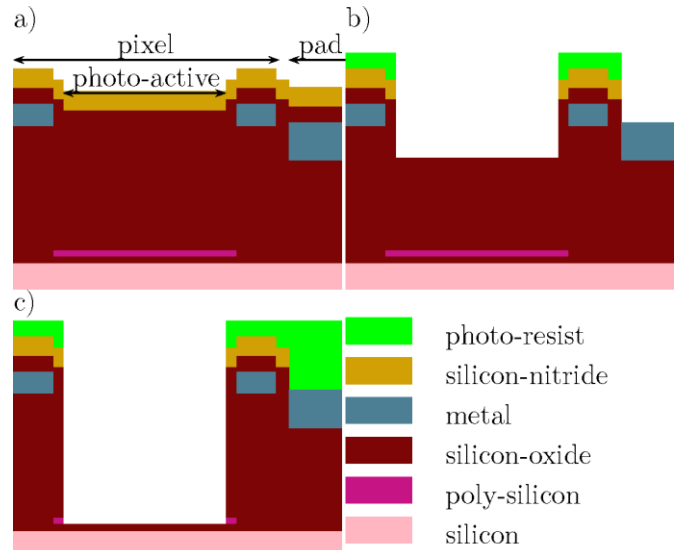


Fig. 1 Schematic illustration of the DOSE process. a) CMOS process until pad opening. b) Photo resist is applied, pad regions are opened together with diode regions lithographically and pad etching is performed. c) Photo resist is reapplied, diode regions are opened lithographically and remaining oxide and stopping layer are etched.

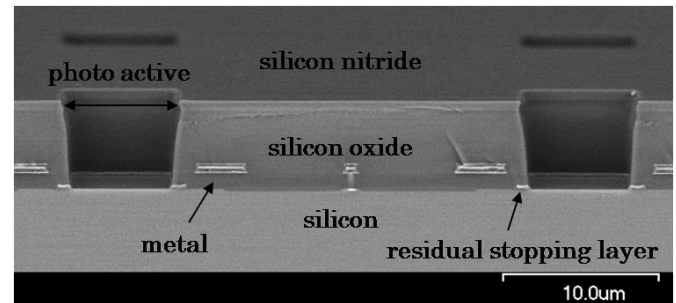


Fig. 2. SEM image of two 7x7  $\mu\text{m}^2$  DOSE photo diodes.

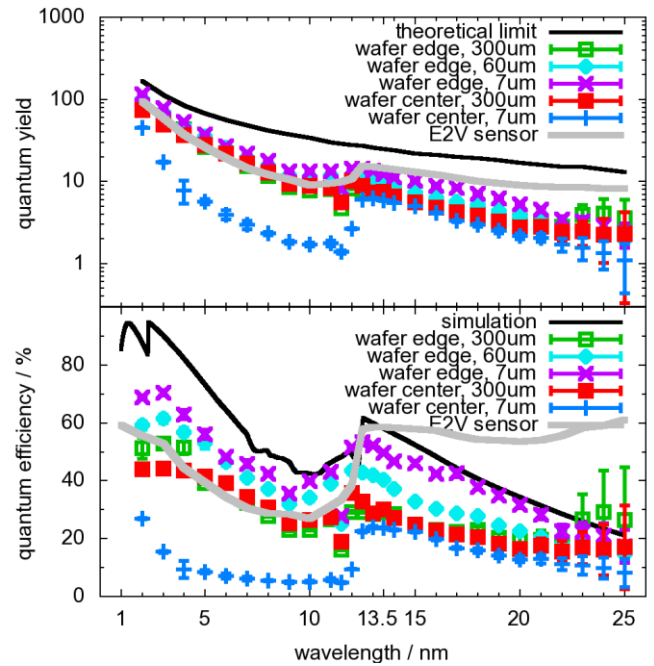


Fig. 3. (Bottom) The quantum efficiency of the DOSE CMOS photo diodes (sizes: 300  $\mu\text{m}$ , 60  $\mu\text{m}$ , 7  $\mu\text{m}$ ) compared to a simulation of approx. 50 nm thermal oxide thickness and a state-of-the-art back-thinned e2v

sensor CCD47-10. (Top) Corresponding quantum yield together with the theoretical limit for an effective bandgap of 3.7 eV.

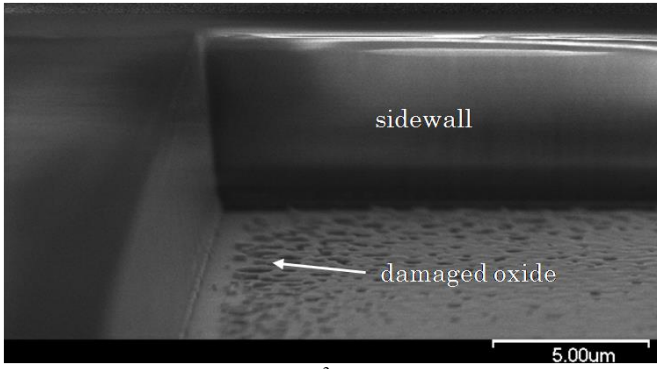


Fig. 4. SEM image of a  $60 \times 60 \mu\text{m}^2$  diode from the wafer edge showing a damaged thermal oxide near the sidewalls.

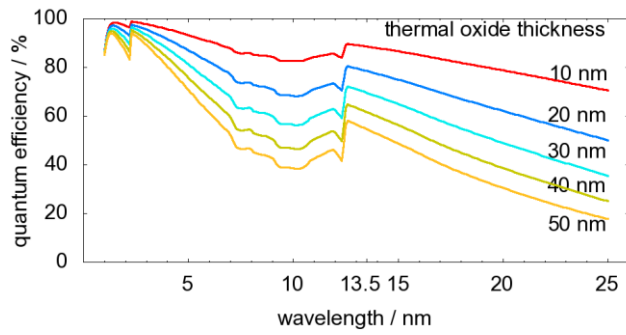


Fig. 5. Quantum efficiency simulation of DOSE photo diodes for different thermal oxide thicknesses as a function of wavelength.